GA–A26665

MAIN CHAMBER PLASMA-WALL INTERACTION STUDIES IN DIII-D IN SUPPORT OF ITER

by
J.G. WATKINS, D.L. RUDAKOV, C.J. LASNIER, A.W. LEONARD,
R.A. PITTS, J.H. YU, T.E. EVANS, R. NYGREN,
P.C. STANGEBY and W.R. WAMPLER

APRIL 2010

GENERAL ATOMICS

DISCLAIMER

GA–A26665

MAIN CHAMBER PLASMA-WALL INTERACTION STUDIES IN DIII-D IN SUPPORT OF ITER

by
J.G. WATKINS[1], D.L. RUDAKOV[2], C.J. LASNIER[3], A.W. LEONARD,
R.A. PITTS[4], J.H. YU[2], T.E. EVANS, R. NYGREN[1],
P.C. STANGEBY[5] and W.R. WAMPLER[1]

This is a preprint of a paper to be presented at the 23rd IAEA Fusion Energy Conference, October 11–16, 2010 in Daejon, Republic of Korea and to be published in Proceedings.

[1]Sandia National Laboratories, Albuquerque, New Mexico
[2]University of California-San Diego, La Jolla, California
[3]Lawrence Livermore National Laboratory, Livermore, California
[4]ITER, Cadarache, France
[5]University of Toronto, Toronto, Ontario, Canada

Work supported in part by
the U.S. Department of Energy
under DE-AC04-94AL85000, DE-FG02-07ER54917,
DE-AC52-07N27344 and DE-FC02-04ER54698

GENERAL ATOMICS ATOMICS PROJECT 30200
APRIL 2010

GENERAL ATOMICS

Recent experiments in DIII-D have examined heat and particle flux profiles to main chamber regions that are of particular concern for the design of the ITER first wall. The first of these are at the high and low field side midplanes where ITER is expected to limit L-mode plasmas during the ramp-up and ramp-down phases of the plasma discharge. The scrape-off layer (SOL) power decay widths during inner wall limited (IWL) L-mode discharges in DIII-D are on the average ~2.5 times larger than those in diverted and upper outer wall limited plasmas, in agreement with the assumptions used in the ITER first wall design. A second important area of concern for main chamber interactions in ITER is at the top of the vessel where a secondary divertor is expected to handle both steady state and ELMing levels of particles and energy. On DIII-D, measurements in H-mode show that the heat flux deposition on this secondary divertor region is 3-4 times broader than that seen at the primary divertor largely due to the effect of ELMs.

The power handling on the limiter is determined by the shaping and the parallel heat flux density characterized by the SOL power flux density e-folding length, λ_q. In the ITER thermal load specifications [1], the limiter phase λ_q is derived from a modified L-mode divertor plasma scaling based mostly on JT-60U and JET results. Here we have used limited plasmas and scanned the main scaling parameters, plasma density, n_e, plasma current, I_p, and power into the SOL, P_{SOL}. Using the near-SOL density and temperature e-folding lengths, λ_n, λ_T, determined from reciprocating Langmuir probe measurements made near the outer midplane, λ_q is derived assuming $T_e = T_i$ in the SOL. The measurements show that λ_n and λ_T are correlated ($\lambda_T \sim 1.2\ \lambda_n$) and both are up to 2.5 times larger in IWL configurations than in lower single null (LSN) [Fig. 1(a)]. In moderate elongation (κ~1.4) IWL discharges, λ_q is nearly constant with I_p, n_e, and power unlike the assumed ITER scaling [Fig. 1(b)]. In LSN discharges with attached outer strike point, IRTV and probe measurements of λ_q agree within a factor of ~2. In IWL discharges, λ_q measurements are consistent with the expectations of a simple SOL power balance. Scaling dependencies of λ_q on the individual discharge parameters do not agree with our data. However, the fact that scaled JT-60U and JET data agree reasonably with the DIII-D measurements supports the strong machine size dependence ($\lambda_q \propto R^2$, where R is the major radius) assumed by the ITER scaling.

ITER will use unbalanced double-null configurations for which a secondary divertor region exists at the top of the vessel and for which first wall design must account. Power fluxes in this

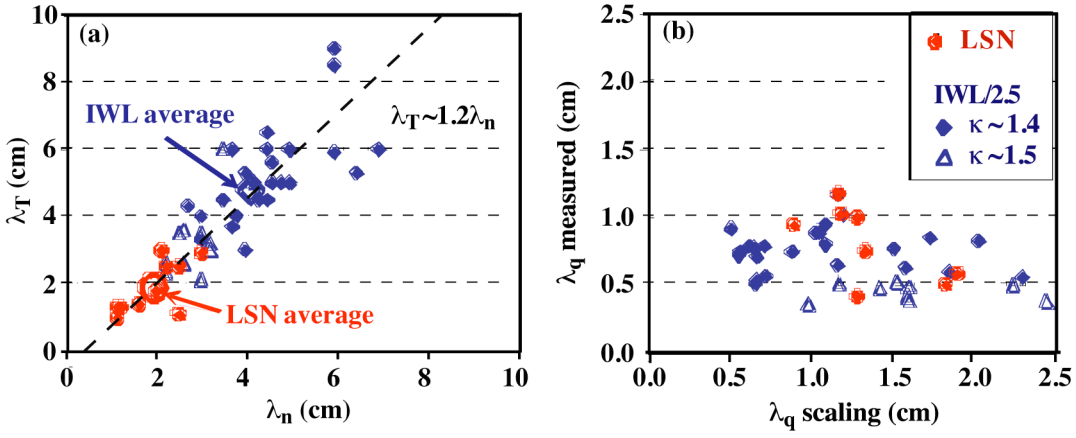

Fig. 1. (a) Near-SOL density and temperature e-folding lengths in IWL and LSN configurations; (b) measured power flux density e-folding length vs that predicted by ITER scaling [1]. Measured IWL data in (b) are divided by 2.5 to be on the same scale with LSN points.

region have not generally been well diagnosed and thermal and particle loads during and between ELMs need to be better characterized in support of the proposed ITER first wall design. For an ITER similar shape with the ion $B \times \nabla B$ drift towards the primary upper x-point, 50% larger core plasma density ($5.0 \rightarrow 7.5 \times 10^{19}$ m^{-3}) resulted in smaller ELMs, less radial transport of particles, and 75% less energy per ELM into the secondary SOL and divertor. Averaged over ELMs, λ_q in the secondary divertor is observed to be 3-4 times broader than typical for the primary divertor. As the magnetic balance shifts more towards the main divertor, the heat and particle flux to the secondary divertor is reduced and the total energy per ELM deposited on the secondary divertor drops proportionally with drsep.

Detailed measurements of the ELM energy and particle deposition footprint on the secondary divertor target plates were made with a fast IR camera, Langmuir probes, and fast response thermocouples embedded 1 cm below the target plate surface. SOL profile and transport measurements were made with reciprocating probes at the outer midplane. Particularly striking are the images from a new fast IR camera that looks down into the secondary divertor showing spiral patterns with multiple peaks during ELMs (Fig. 2). These patterns are consistent with transport due to radial propagation of filaments that were also measured by a reciprocating probe and a fast framing camera at the outer midplane. Carbon (C^{13}) deposition measurements have also been performed in the secondary divertor for tritium inventory and impurity estimates.

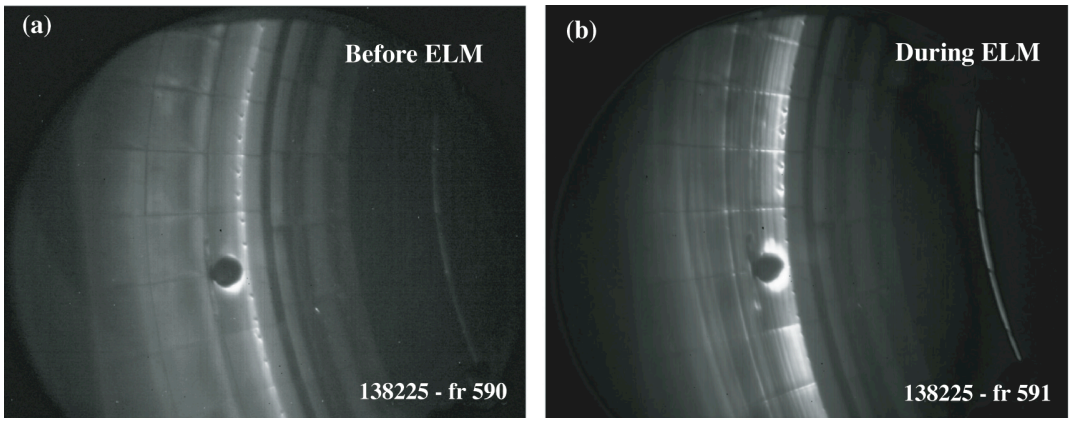

Fig. 2. Fast IR camera images looking down at the toroidal strike point in the secondary divertor before and during an ELM.

This work was supported in part by the US Department of Energy under DE-AC04-94AL85000, DE-FG02-07ER54917, DE-AC52-07N27344, DE-FC02-04ER54698, and the Collaborative Research Opportunities grant from the National Sciences and Engineering Research Council of Canada.

[1] A. Loarte, *et al.,* Proc. 22nd IAEA Fusion Energy Conf., IT/P6-13 (2008).